Available online at www.sciencedirect.com
ScienceDirect
Diamond & Related Materials 17 (2008) 262–269
DIAMOND AND RELATED MATERIALS
www.elsevier.com/locate/diamond

X-ray topography studies of dislocations in single crystal CVD diamond

M.P. Gaukroger [a], P.M. Martineau [a,*], M.J. Crowder [a], I. Friel [b], S.D. Williams [b], D.J. Twitchen [b]

[a] DTC Research Centre, Belmont Road, Maidenhead, Berkshire, SL6 6JW, UK
[b] Element Six, King's Ride Park, Ascot, Berkshire, SL5 8BP, UK

Received 29 August 2007; received in revised form 20 November 2007; accepted 12 December 2007
Available online 23 December 2007

Abstract

X-ray topography has been used to study single crystal diamond samples homoepitaxially grown by microwave plasma-assisted chemical vapour deposition (CVD) on high pressure high temperature (HPHT) and CVD synthetic diamond substrates. Clusters of dislocations in the CVD diamond layers emanated from points at or near the interface with the substrate. The Burgers vectors of observed dislocations have been determined from sets of {111} projection topographs. Dislocations have line directions close to the [001] growth direction and are either edge or 45° mixed dislocations. Where groups of dislocations originated at isolated points they tended to be of the edge variety. Where the substrate surface was deliberately damaged before growth, two sets of dislocations were observed to have propagated from each line of damage and there was a tendency for dislocations to be of the 45° mixed variety with a component of their Burgers vector parallel to the polishing direction. It is demonstrated that X-ray topography can be used to deduce the growth history of CVD synthetic diamond samples produced in multiple growth stages.

Keywords: Defect characterization; Single crystal growth; Homoepitaxy

1. Introduction

Although there have been many reports of studies of point defects in single crystal CVD diamond, there have been relatively few reported investigations of extended structural defects, such as dislocations and stacking faults. X-ray topography and transmission electron microscopy (TEM) are the two most common techniques used for studying extended defects. X-ray topography offers a non-destructive method of studying the dislocation content of the complete volume of moderately large crystals that have relatively low dislocation densities. In contrast, TEM involves destructively cutting and thinning specimens and its small sampling volume means that it is most likely to give useful information in regions of crystal with relatively high dislocation density.

Evidence of dislocations may also be observed in cathodoluminescence topographs and photoluminescence images of diamond. In some cases dislocations give rise to characteristic blue streaks [1] in such images and they may also have a quenching effect on impurity related luminescence. X-ray and cathodoluminescence topography have been extensively applied to natural diamond by Lang and others [2,3].

Controlling impurity concentrations is very difficult in HPHT synthesis but CVD can be used to produce diamond material of high purity or with controlled doping [4–10]. For this reason, CVD diamond has potential applications in electronics which are not open to HPHT-grown diamond. Extended structural defects, such as dislocations or stacking faults, are likely to affect the suitability of material for such applications but there has been no systematic research published on extended defects in single crystal CVD diamond.

Gemmologists have an interest in the extended structural defect content of diamond material from different origins. Understanding differences can, for example, be a useful aid in the identification of natural and synthetic diamond. Natural type IIa diamond contains relatively high densities (up to 10^9 cm^{-2}) of dislocations [11] resulting from plastic deformation and arranged either in slip bands or in geometric arrangements resulting from polygonisation [12,13]. Although X-ray techniques

* Corresponding author.
E-mail address: philip.martineau@dtc.com (P.M. Martineau).

0925-9635/$ - see front matter © 2007 Elsevier B.V. All rights reserved.
doi:10.1016/j.diamond.2007.12.036

are not extensively applied by gemmologists, recent research has shown that X-ray topography can add useful support for identifying the origin of diamond material. Martineau et al. [13] found that dislocations in homoepitaxial CVD diamond layers tend to nucleate at or near the interface with their substrate. They also found that they have line directions that are close to perpendicular to the local growth surface and that, as a result, the strain-related birefringence shows a characteristic anisotropy, being much more obvious for a viewing direction parallel to the growth direction. In a study of CVD diamond grown epitaxially on a {001} diamond substrate, Mora et al. [14] recorded TEM images of straight dislocations with line directions parallel to the growth direction and reported that some of these dislocations had a/2<110> Burgers vectors. Fujita et al. [15,16] have carried out *ab initio* modelling studies of two types of <001> dislocation: a 45° mixed dislocation and a pure edge dislocation.

Here we report the results of an X-ray topography study of dislocations in {001} CVD diamond grown epitaxially on {001} substrates.

2. Experimental details

The four homoepitaxial diamond samples studied here were grown using microwave plasma CVD on {001} type Ib high pressure high temperature-grown synthetic diamond substrates in the form of parallel-sided plates with dimensions in the region of 3 mm × 3 mm × 0.5 mm. The crystallographic orientation of the six faces of these substrates was {100}. Substrates surfaces were polished to a high standard on a diamond impregnated scaife but for samples B and C the upper surface of the substrate was subsequently deliberately damaged by rough polishing along the [010] direction.

The substrates of samples A, B and C were removed after growth and in each case six {100} faces were polished. The final sample dimensions are given in Table 1. Sample D was made up of material from three growth runs. First a CVD layer was grown on a type Ib substrate and cross-sectioned to produce a vertically cut {100} CVD plate. This was subsequently used as a substrate in the second growth run. The resulting sample was then cross-sectioned to produce a vertically cut {100} plate which was subsequently used as a substrate in the third growth run. Finally, the resulting material was processed into a sample with six {100} faces that contained portions grown in each of the three successive growth stages with orthogonal growth directions.

Table 1
Sample details

Sample label	Dimensions (mm)	Notes
A	4.32 × 3.54 × 1.34	Grown on a well polished substrate
B	3.40 × 3.08 × 0.70	Grown on a deliberately damaged substrate
C	3.47 × 3.18 × 0.65	Grown on a deliberately damaged substrate
D	3.60 × 2.94 × 3.74	Grown in three stages with orthogonal growth directions

The post-growth polishing into parallel-sided samples allowed the recording of crossed polariser optical micrographs showing birefringence resulting from strain in the CVD layer. It also allowed photoluminescence images to be recorded for CVD material close to the substrate/sample interface. Such images were recorded using a DiamondView instrument that exposes samples to above band gap UV radiation to excite surface luminescence and can give information about spatial variations in the intensity of luminescence emanating from point defects or dislocations.

X-ray topographs were recorded using a Lang camera fitted to a rotating anode X-ray generator having a molybdenum target, zirconium filter and 0.2 mm × 0.2 mm apparent source size. The operating conditions of 40 kV, 40 mA produced a bright source of molybdenum $K\alpha_1$ X-rays at 17.4 keV. A 250 μm slit collimator was used at a distance of 0.7 m from the source. Preliminary X-ray topographs were generated rapidly on dental film before high quality topographs, requiring longer exposure times, were recorded on nuclear plates (Ilford L4) and processed using standard techniques.

Section topographs were recorded using a {533} reflection. With molybdenum $K\alpha_1$ radiation, use of a {533} reflection allows samples to be set up in such a way that the plane sampled by the X-ray beam is within 2° of a {100} plane. It also allows topographs to be recorded with relatively little projection distortion because, at 81.37°, 2θ for the Bragg condition is fairly close to 90°. Exposure times were typically 1 h.

To provide information about the dislocations throughout a sample, projection topographs were recorded by translating the sample through the beam in order to expose its complete volume. The film was simultaneously translated to keep it in the same position relative to the sample. Exposure times varied between 1 and 4 h, depending on sample size, intensity of the reflection used and the degree of lattice perfection.

For Burgers vector analysis, projection topographs were recorded for four different <111> reflections. Dislocations in diamond generally have <110> Burgers vector. The six different <110> directions are given by the lines along which two different {111} planes intersect. To a good approximation, a dislocation is invisible in a given X-ray topograph if its Burgers vector lies parallel to the atomic layers responsible for diffraction. This means that for a set of four topographs, each generated using a different <111> reflection, a given dislocation with a <110> Burgers vector should be present in two topographs but absent from the other two topographs, with the Burgers vector given by the line of intersection of the diffracting planes for the latter two topographs.

Use of <111> diffraction had other advantages. For diamond, the {111} reflection gives the highest intensity and the exposure time was therefore minimised. The <111> reflections provide four equivalent views of the parallel-sided (001) plates studied in this research. With molybdenum $K\alpha_1$ X-rays, in each case the topograph presents a view in a direction that is inclined at 25.34° to the normal to the major faces of the sample. This angle is large enough to allow the entry and exit points of dislocations with line directions close to [001] to be clearly distinguished but it is small enough not to give rise to significant confusion from overlapping lines.

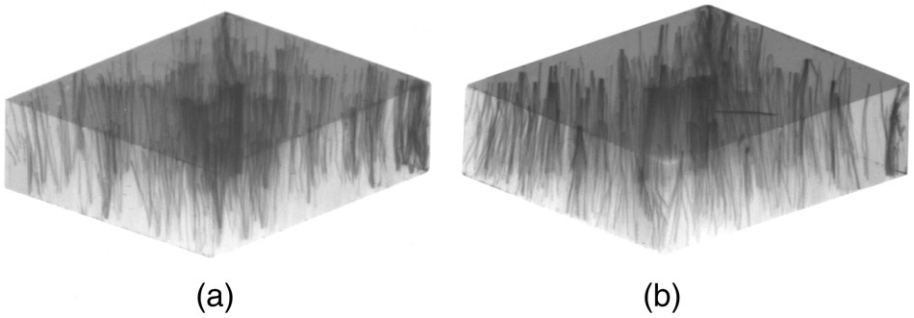

Fig. 1. {004} projection topographs of a free-standing layer of single crystal CVD diamond (sample A) with the surface closest to the final growth surface facing (a) upwards and (b) downwards.

A computer programme, written in Visual Basic, was developed to aid the matching of dislocation-related contrast seen in four <111> projection topographs of a given sample. A coordinate system was defined using one corner and three edges of the parallel-sided sample under investigation. The software was then used to identify the pairs of coordinates corresponding to the points where individual lines broke the upper and lower surfaces of the sample. In this way lists of line positions and contrast strength were built up for each of the recorded topographs. Matching of coordinate pairs in different topographs within a set tolerance was taken as an indication that the same line had been imaged. A table was then created to list for each line which <111> reflection gave invisibility/visibility.

3. Results

3.1. Sample A

Sample A was initially selected as a test sample for the development of X-ray topography techniques suitable for developing understanding of the dislocations found in single crystal CVD diamond. Fig. 1 shows {004} projection topographs taken from either side of the (001) plate. These topographs illustrate the spatial distribution of the dislocation-related features within the sample.

In order to characterize the dislocation-related features in sample A, four {111} topographs (Fig. 2) were recorded and analysed using the software described above. 346 dislocation

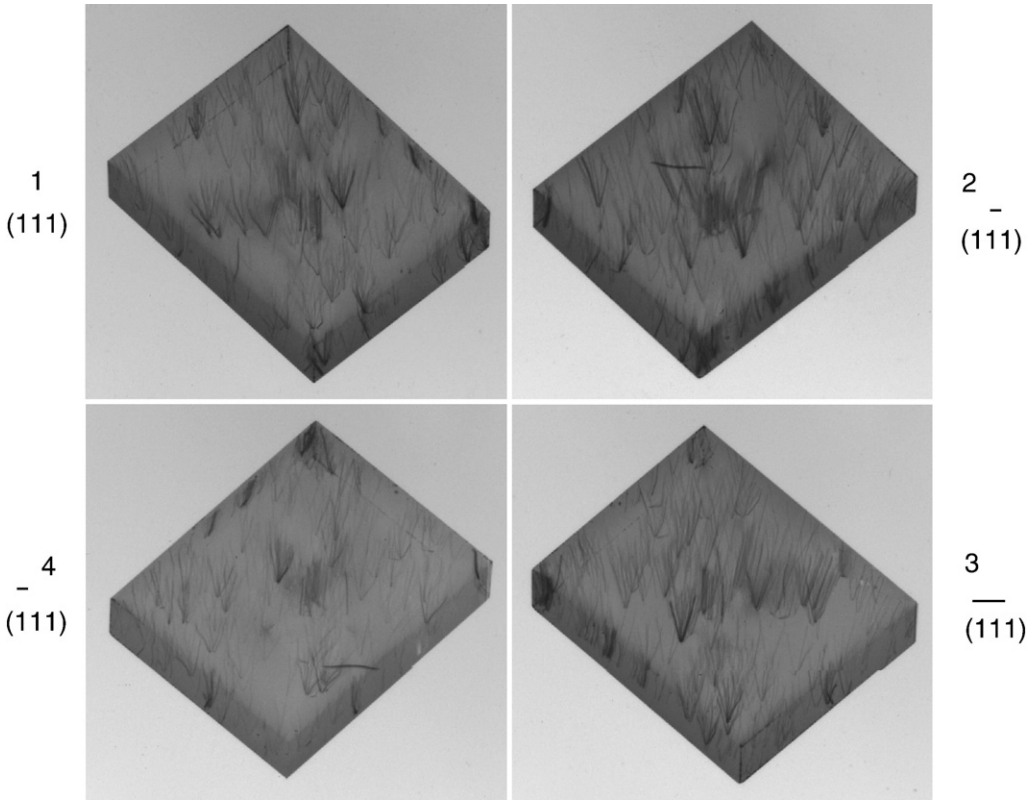

Fig. 2. Four {111} projection topographs of sample A used for Burgers vector analysis.

Table 2
Results of Burgers vector analysis for sample A

Burgers vector	Number of lines
[110]	11
[1$\bar{1}$0]	11
[101]	4
[0$\bar{1}$1]	6
[$\bar{1}$01]	5
[0$\bar{1}\bar{1}$]	8

lines were identified in one or more topographs and of these 45 were absent in only two topographs allowing the Burgers vector to be determined. 23 lines were observed in all four topographs. 22 lines were absent in only one topograph. 98 lines appeared to absent in three topographs. It is possible that image contrast was too weak in some cases to reveal all the lines and in other cases, where one line was masked by another, it was not possible to determine line positions and complete the line matching.

There were 45 instances in which the Burgers vector could be determined and in these cases the line direction was close to [001]. In 22 cases the Burgers vector lay in the plane of the plate sample indicating that these were edge dislocations. In half the cases the Burgers vector was [110] or [1$\bar{1}$0]. In the 23 remaining cases the Burgers vector had a direction that was inclined at 45° to the plane of the plate, indicating mixed dislocations which are not purely edge or screw dislocations. These results are listed in the Table 2.

3.2. Samples B and C

Samples B and C were chosen for a study of how the dislocation content of a single crystal CVD diamond layer is affected by damage at the surface of the substrate on which it is grown. Fig. 3 shows an optical micrograph recorded using cross-polarisers, a DiamondView UV-excited luminescence image and a {533} X-ray section topograph recorded for sample B. All three images show linear features relating to the dislocations nucleating on the <100> damage tracks created on the upper surface of the substrate before growth. The orange luminescence seen in the DiamondView image is from nitrogen-vacancy defects that were incorporated during growth as a result of the presence of a low concentration of nitrogen in the growth environment. The orange lines seen in the DiamondView image are a result of different uptake of these nitrogen-related defects on the risers and terraces of steps that formed on the growth surface [13]. The blue lines correspond to regions of high dislocation density.

Fig. 4 shows {533} section topographs recorded for sample B, using (a), (b) cross-sectional and (c) plan view geometries. The dotted line shows the approximate position of cross-sections (a) and (b) in the plan view image. Allowing for projection distortion in both topographs, there is good correspondence between linear features observed in the plan view and V-shaped features in the cross-section. In Fig. 4(a) dimples are visible at the top of the V-shaped features. The region of the topograph where these dimples are seen corresponds to the side of the sample closest to the final growth surface. Higher magnification revealed that small pimples exist in the region of the topograph at the point of each V-shaped feature, despite the fact that both the corresponding surfaces of the sample had been polished flat. Fig. 4(b) shows a similar topograph recorded with the sample rotated by 180° about the sample's [001] growth direction. Note the reversal of the direction of deviation at these V-shaped features from the lines in the topograph corresponding to the upper and lower surface of the sample. This reversal suggests the material within the V-shaped regions is tilted, relative to the surrounding crystal, about an axis parallel to the long dimension of the cross-section. The magnitude of this deviation was measured and, knowing the approximate sample-to-film distance, the lattice misalignment angle calculated to be 10^{-3} radians (approximately 0.06°).

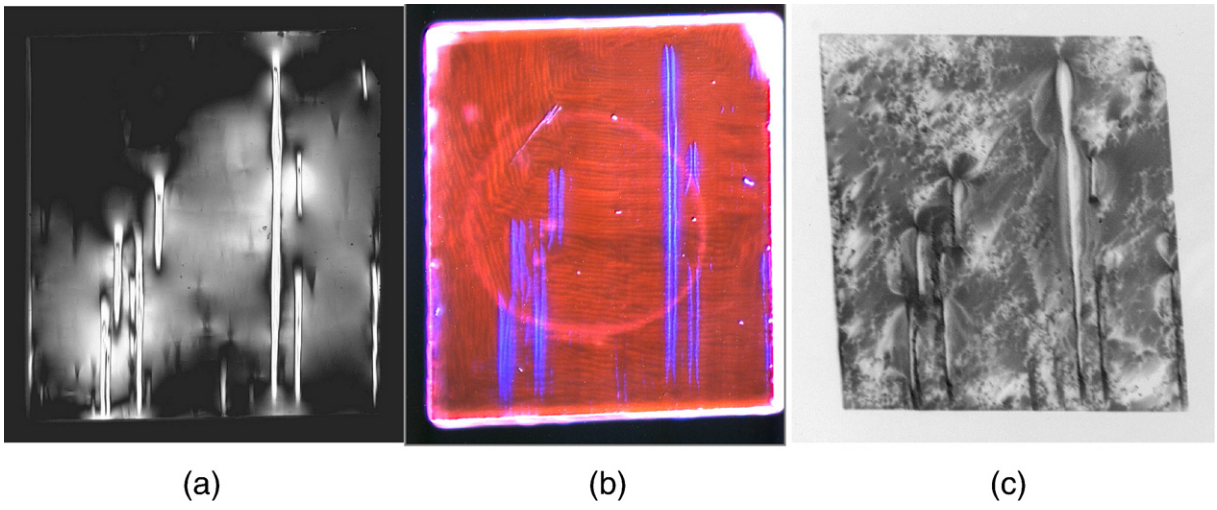

Fig. 3. (a) Crossed-polariser, (b) DiamondView and (c) {533} X-ray section topograph images of a layer of single crystal CVD diamond (sample B) after removal from the substrate on which it was grown. The substrate was deliberately damaged prior to growth. The circular feature seen in the DiamondView image is the holder on which the sample was mounted.

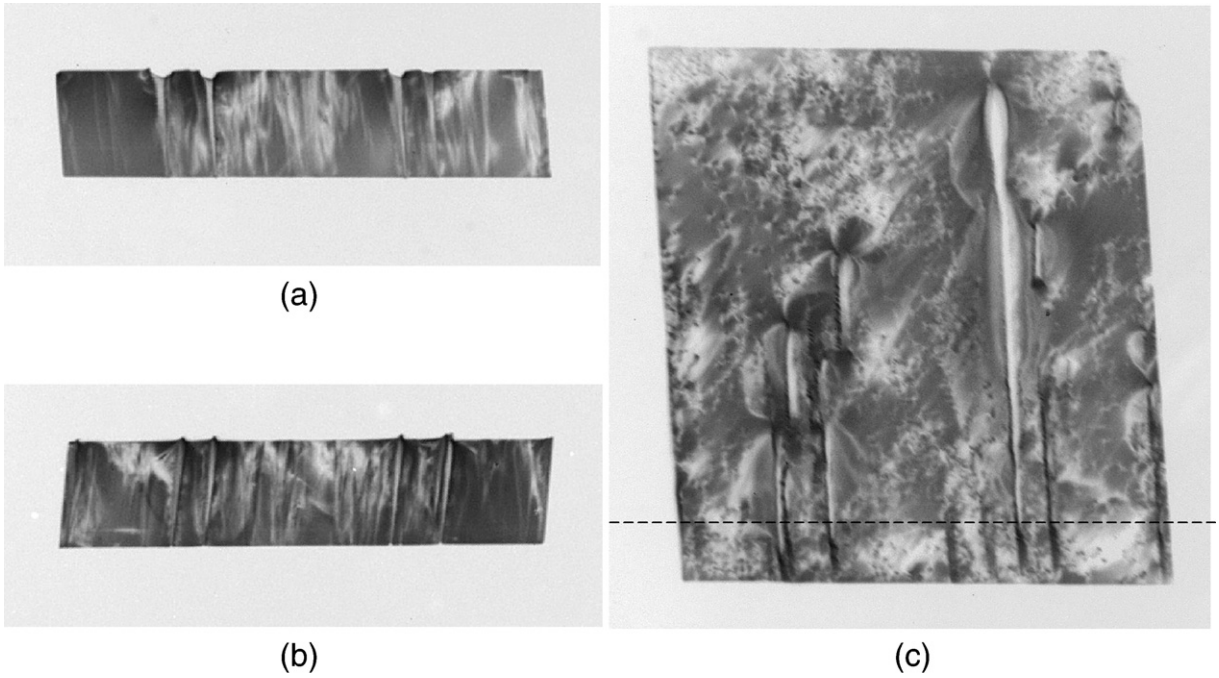

Fig. 4. {533} section topographs of sample B. (a) Cross-sectional geometry, (b) cross-sectional geometry with the sample rotated by 180° about a vertical axis and (c) plan view geometry.

The {111} projection topographs used for Burgers vector determination for sample C are shown in Fig. 5. 196 lines were identified in one or more topographs. 67 were absent in only two topographs, allowing the Burgers vector to be determined. 4 lines were observed in all four topographs, 13 lines in three and 112 lines appeared to be present in only one topograph.

For the 67 lines for which the Burgers vector could be determined, the results are given in Table 3. These lines lay close to [001]. In 13 cases the Burgers vector lay in the (001)

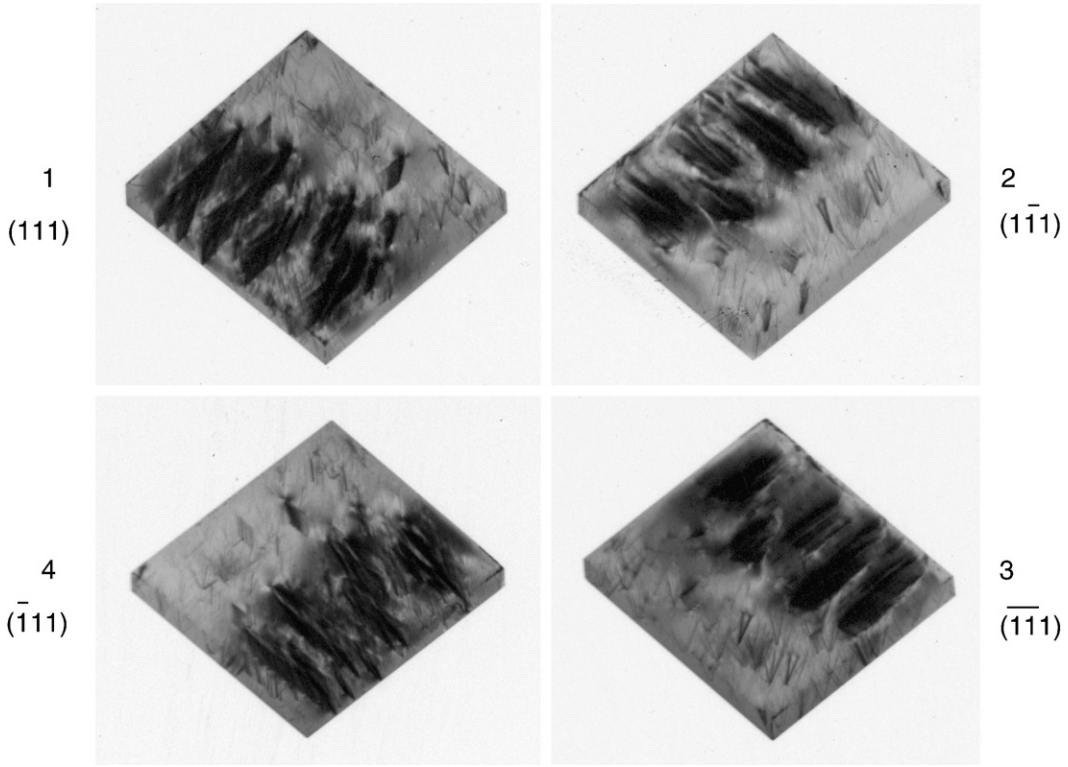

Fig. 5. Four {111} projection topographs of sample C used for Burgers vector analysis.

Table 3
Results of Burgers vector analysis for sample C

Burgers vector	Number of lines
[110]	6
[1$\bar{1}$0]	7
[101]	8
[0$\bar{1}$1]	31
[$\bar{1}$01]	10
[0$\bar{1}$1]	5

plane, indicating edge dislocations, with an approximately equal distribution between [110] and [1$\bar{1}$0]. In the 54 remaining cases the Burgers vector had a direction that was inclined at 45° to (001), indicating 45° "mixed" dislocations. Note the asymmetry of distribution of Burgers vectors for the mixed dislocations. The majority were found to have a [011] Burgers vector and these dislocations tended to be grouped along lines with [010] projections onto the (001) plane. This is parallel to the linear features, seen in Figs. 3, 4 and 5, that are known to result from polishing damage.

3.3. Sample D

Fig. 6 is a {111} projection topograph of a single crystal CVD diamond sample containing portions grown in three stages with mutually perpendicular growth directions. In this topograph, the different portions corresponding to different growth stages can be identified because the dislocation-related lines indicate the growth direction. The part corresponding to the first stage of growth is in the lower foreground. The second stage growth forms the base of the sample, with its growth direction towards the back of the topograph. The material from the third stage of growth forms the bulk of the sample.

4. Discussion

The dislocations in natural type IIa diamond are dominantly a result of plastic deformation and therefore tend to lie in the {111} glide plane. For example, the dominant line directions found in a TEM study of brown type IIa natural diamond [11] were <110> and <112>. In contrast, the majority of dislocations observed in this study have a near-[001] line direction and are therefore "grown-in" dislocations. It is likely that, during growth, these dislocations had a tendency to propagate in the local growth direction because this minimized their total energy. Variations in the local growth direction, such as passing growth steps with risers tilted away from [001], would be expected to influence the line direction. Similarly, local strain fields, such as those resulting from near-by dislocations, could also play a role in causing deviations.

It has been difficult to determine in which cases the line contrast relates to individual dislocations and which cases it corresponds to groups of dislocations. The width of many of the observed lines exceeds the extent of the strain field expected from a single dislocation [17] and this suggests that in many cases groups of dislocations are being observed. The large range in contrast also suggests groups of dislocations are responsible for at least the lines showing strongest contrast. There are, however, many instances of lines for which contrast is absent in two {111} topographs, allowing the Burgers vector to be determined. In these cases, if the line results from a group of dislocations, the majority of those dislocations must have the same Burgers vector.

In cases where dislocations are absent in two {111} topographs related by a 180° rotation of the sample, the Burgers vector lies in one of two <110> directions in the (001) plane of the sample. Since the dislocation line directions are close to [001], the corresponding dislocations are edge dislocations over

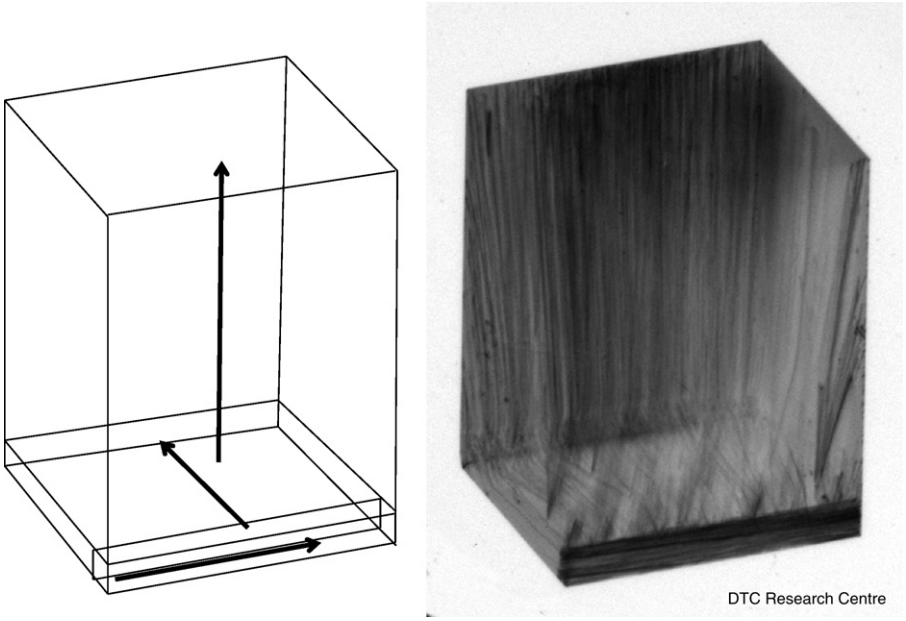

Fig. 6. {111} projection topograph of a block of single crystal CVD diamond produced in three sequential growth stages for which the <001> growth directions were orthogonal to each other, as illustrated in the accompanying diagram.

much of their length. Where they are absent in two {111} topographs related by a 90° sample rotation, the Burgers vector lies on one of the four <110> directions inclined at 45° to the [001] growth direction, suggesting that these are 45° mixed dislocations over the majority of their length.

Fujita et al. [15,16] have carried out *ab initio* modelling studies of two types of <001> dislocation in diamond: mixed 45° and pure edge dislocations. Their results suggest that the mixed 45° <001> dislocation has a lower energy than either a pure edge dislocation or a kinked dislocation that consists of short <110> edge and screw segments. In this study we have identified both edge and 45° mixed dislocations and our results suggest that their relative number densities depend on the relative number densities of the sources that give rise to these different kinds of dislocation. For example, where the substrate surface shows polishing damage mixed 45° <001> dislocation appear to dominate but when a substrate is well polished approximately equals numbers of the two kinds of dislocation can result.

In many instances dislocations are observed as clusters of four or more lines diverging from isolated points at the interface between the CVD layer and the substrate on which it was grown, and propagating in a direction close to the [001] growth direction. In cases where only four lines are observed to emanate from a given point, these deviate from [001] in such a way that their projections onto the (001) plane lie along <110> directions. Only two of these four lines are visible in each {111} topograph. In most cases, those with projections along [110] or $[\bar{1}\,\bar{1}0]$ have $[1\bar{1}0]$ Burgers vectors, and those with projections along $[1\bar{1}0]$ or $[\bar{1}10]$ have [110] Burgers vectors. These clusters of lines therefore seem to be made up predominantly of edge dislocations.

In heteroepitaxial growth systems a network of dislocations often forms at the interface between the substrate and the layer grown on it. Such a network can help to accommodate the difference in lattice parameter. In homoepitaxial growth of diamond by CVD, although most dislocations are formed at or near the interface [13], we have found no evidence of such dislocation networks. The dislocations formed at the interface immediately propagate along the growth direction as growth proceeds. Since dislocations cannot terminate within a single crystal material, it follows that the clusters of dislocations that emanate from isolated points at the interface must have no net Burgers vector. Where there are just four dislocations forming a cluster, the simplest configuration that fits our experimental observations would be composed of two dislocation dipoles.

In the topographs of samples B and C, two sets of dislocations diverge from each surface damage track on the substrate. In each case, the material between the two sets of dislocations has a slight angular misalignment with respect to the surrounding crystal. The Burgers vector analysis indicates that mixed dislocations dominate and that the majority of these have [011] Burgers vector. The damage created on the surface of the substrate was achieved by rough polishing in the [010] or $[0\bar{1}0]$ direction but it is not known in which of these two direcions the scaife moved across the surface. It is clear that dislocation lines propagating from such damage tracks have a tendency to contain 45° mixed dislocations having an edge component of their Burgers vector lying along the direction of polishing. It is well known [18] that, during polishing of diamond surfaces, "clatter tracks" consisting of lines of short cracks can form. It is probable that such clatter tracks on the damaged substrate surface led to the formation of these dislocations during the early stages of growth. Analysis of the section topographs shown in Fig. 4 suggests that the material above such clatter tracks is slightly tilted with respect to the surrounding crystal and the Burgers vector of the dominant variety of mixed dislocation that we have associated with substrate damage appears to have a screw component in a direction that would accommodate such a tilt. A spacing of approximately 1000 Burgers vectors between adjacent dislocations would produce the observed angular misalignment of 0.001 radians.

It has previously been shown that X-ray topography can be used to distinguish between natural and CVD synthetic diamond [6]. It is clear from the topograph of sample D that X-ray topography is also an effective technique for identifying the growth history of CVD synthetic diamond samples which have been grown in a series of stages. For substrate use, a vertically cut cross-sectional slice has the advantage, relative to a horizontally cut CVD plate, that a smaller proportion of its dislocations propagate into a layer grown on it. This is a consequence of the fact that fewer of them break the surface on which growth takes place, simply because their line direction is nominally parallel to it. The topograph does however contain evidence that some of the dislocations break the surface of the cross-sectional slice and then propagate in the new growth direction at 90° to the original growth direction.

5. Conclusions

Dislocations in {001} homoepitaxial CVD diamond can be classified in terms of their line direction and Burgers vector by means of X-ray topography. Dislocation lines have been seen to generate large differences in contrast in X-ray topographs, suggesting that in many cases they correspond to bundles of dislocations. Clusters of dislocations have been seen to diverge from isolated points on the upper surface of the substrate. Such clusters tend to be made up of <001> edge dislocations.

Dislocations originating at polishing damage at a {001} substrate surface, tend to be 45° mixed dislocations with a Burgers vector component parallel to the polishing direction. Substrate polishing damage can cause significant birefringence in homoepitaxially grown CVD diamond layers because it causes the formation of such dislocations. It is proposed that the screw component of these mixed dislocations accommodates the observed angular misalignment of regions above substrate polishing damage.

We have demonstrated how X-ray topography can be used to deduce the growth history of CVD synthetic diamond samples produced in multiple growth runs. It should be clear from this study that X-ray topography is a powerful diagnostic tool that can be used to develop understanding of factors limiting crystal quality.

Acknowledgements

The authors would like to thank C.J. Kelly and M.J. Sheehy for the skillful polishing of the samples studied in this work. They also thank J. Härtwig for useful discussions.

References

[1] I. Kiflawi, A.R. Lang, Phila. Mag. 33 (4) (1976) 697.
[2] A.R. Lang, in: J.E. Field (Ed.), The Properties of Diamond, Academic Press, London, 1979, p. 425.
[3] A.R. Lang, M. Moore, J.C. Walmsley, in: J.E. Field (Ed.), The Properties of Natural and Synthetic Diamond, Academic Press, London, 1992, p. 215.
[4] J. Isberg, J. Hammersberg, E. Johansson, T. Wikstrom, D.J. Twitchen, A.J. Whitehead, S.E. Coe, G.A. Scarsbrook, Science 297 (5587) (2002) 1670.
[5] T. Teraji, T. Ito, J. Cryst. Growth 271 (2004) 409.
[6] M. Suzuki, H. Yoshida, N. Sakuma, T. Ono, T. Saki, M. Ogura, H. Okushi, S. Koizumi, Diamond and Related Materials 13 (2004) 198.
[7] S. Koizumi, M. Suzuki, Phys. Status Solidi (A) 203 (13) (2006) 3358.
[8] A. Tallaire, J. Achard, F. Silva, R.S. Sussmann, A. Gicquel, Diamond and Related Materials 14 (2005) 249.
[9] J. Achard, F. Silva, A. Tallaire, X. Bonnin, G. Lombardi, K. Hassouni, A. Gicquel, J. Phys. D: Appl. Phys. 40 (2007) 6175.
[10] N. Tranchant, M. Nesladek, D. Tromson, Z. Remes, A. Bogdan, P. Bergonzo, Phys. Status Solidi (A) 204 (9) (2007) 3023.
[11] B. Willems, P.M. Martineau, D. Fisher, J. Van Royen, G. Van Tendeloo, Phys. Status Solidi 203 (12) (2006) 3076.
[12] N. Sumida, A.R. Lang, Phila. Mag. A 43 (5) (1981) 1277.
[13] P.M. Martineau, S.C. Lawson, A.J. Taylor, S.J. Quinn, D.J.F. Evans, M.J. Crowder, Gems. Gemol. 40 (1) (2004) 2.
[14] A.E. Mora, J.W. Steeds, J.E. Butler, C.-S. Yan, H.K. Mao, R.J. Hemley, D. Fisher, Phys. Status Solidi (A) 202 (15) (2005) 2943.
[15] N. Fujita, A.T. Blumenau, R. Jones, S. Oberg, P.R. Briddon, Phys. Status Solidi (A) 203 (12) (2006) 3070.
[16] N. Fujita, A.T. Blumenau, R. Jones, S. Oberg, P.R. Briddon, Phys. Status Solidi (A) 204 (7) (2007) 2211.
[17] J.P. Hirth, J. Lothe, Theory of Dislocations, Second Edition, Krieger Publishing Co., Florida, 1982, p. 59.
[18] J. Wilks, E. Wilks, Properties and Applications of Diamond, Butterworth-Heinemann, Oxford, 1991, p. 254.